NANO LETTERS

xxxx
Vol. 0, No. 0
A−E

Toward Full Spatiotemporal Control on the Nanoscale

Maxim Durach, Anastasia Rusina, and Mark I. Stockman*

Department of Physics and Astronomy, Georgia State University, Atlanta, Georgia 30303

Keith Nelson

Department of Chemistry, MIT, Cambridge, Massachusetts 02139

Received July 16, 2007; Revised Manuscript Received August 8, 2007

ABSTRACT

We introduce an approach to implement full coherent control on nanometer length scales. It is based on spatiotemporal modulation of the surface plasmon polariton (SPP) fields at the thick edge of a nanowedge. The SPP wavepackets propagating toward the sharp edge of this nanowedge are compressed and adiabatically concentrated at a nanofocus, forming an ultrashort pulse of local fields. The profile of the focused waveform as a function of time and one spatial dimension is completely coherently controlled.

Two novel areas of optics have recently attracted a great deal of attention: nanooptics and ultrafast optics. One of the most rapidly developing directions in ultrafast optics is quantum control in which coherent superpositions of quantum states are created by excitation radiation to control the quantum dynamics and outcomes.[1−4] Of special interest are coherently controlled ultrafast phenomena on the nanoscale where the phase of the excitation waveform along with its polarization provides a functional degree of freedom to control the nanoscale distribution of energy.[5−11] Spatiotemporal pulse shaping permits one to generate dynamically predefined waveforms modulated both in frequency and in space to focus ultrafast pulses in the required microscopic spatial and femtosecond temporal domains.[12,13]

In this Letter, we propose and theoretically develop a method of full coherent control on the nanoscale where a spatiotemporally modulated waveform is launched in a graded nanostructured system, specifically a wedge. Its propagation from the thick (macroscopic) to the thin (nanoscopic) edge of the wedge and the concurrent adiabatic concentration provide a possibility to focus the optical energy in *nanoscale* spatial and femtosecond temporal regions. Our method unifies three approaches that individually have been developed and experimentally tested. The coupling of the external radiation to the surface plasmon polaritons (SPPs) propagating along the wedge occurs through an array of nanoobjects (nanoparticles or nanoholes) that is situated at the thick edge of the wedge. The phases of the SPPs emitted (scattered) by individual nanoobjects are determined by a spatiotemporal modulator. The nanofocusing of the SPPs occurs due to their propagation toward the nanofocus and the concurrent adiabatic concentration.

The coupling of the external radiation to SPPs and their nanofocusing have been observed; see, e.g., refs 14,15. The second component of our approach, the spatiotemporal coherent control of such nanofocusing, has been developed.[12,13] The third component, the adiabatic concentration of SPPs, also has been recently observed.[16,17] The idea of adiabatic concentration has been proposed in refs 18,19 (see also ref 20) and further developed theoretically[21,22] It is based on adiabatic following by a propagating SPP wave of a graded plasmonic waveguide, where the phase and group velocities decrease while the propagating SPP wave is adiabatically transformed into a standing surface plasmon (SP) mode. A new quality that is present in our approach is a possibility to arbitrary move the nanofocus along the nanoedge of the wedge. Moreover, it is possible to superimpose any number of such nanofoci simultaneously and, consequently, create any distribution of the nanolocalized fields at the thin edge of the wedge.

Consider first the adiabatic concentration of a plane SPP wave propagating along a nanowedge of silver,[23] as shown in Figure 1a; the theory is based on the Wentzel−Kramers−Brillouin (WKB) or quasiclassical approximation, also called the eikonal approximation in optics,[24] as suggested in refs 18. The propagation velocity of the SPP along such a nanowedge is asymptotically proportional to its thickness. Thus when a SPP approaches the sharp edge, it slows down and asymptotically stops. In a real system with a sharp edge of finite thickness (below we consider a 4 nm limit, well

* Corresponding author. E-mail: mstockman@gsu.edu, homepage: http://www.phy-astr.gsu.edu/stockman.

10.1021/nl071718g CCC: $37.00
Published on Web 08/30/2007

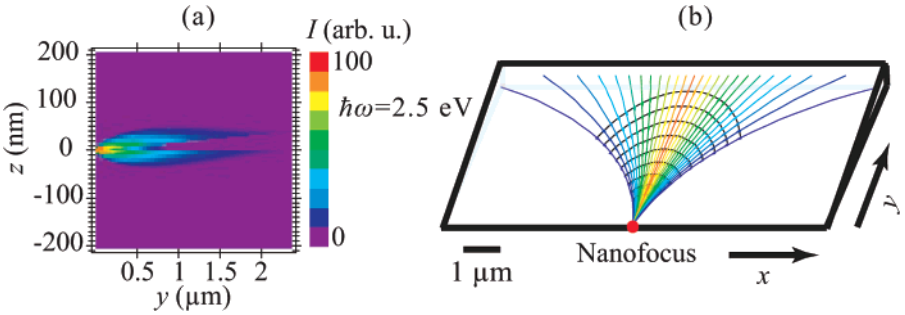

Figure 1. (a) Illustration of adiabatic concentration of energy on the wedge. The distribution of local field intensity I in the normal plane of propagation of SPPs (the yz plane). The intensity in relative units is color coded with the color scale bar shown to the right. This intensity distribution is obtained after eq 4. (b) Trajectories of SPP rays propagating from the thick to sharp edge of the wedge. The initial coordinate is coded with color. The black curves indicate lines of equal phase (SPP wave fronts).

within the achievable range), there is very substantial slowing down, nanofocusing, and increase in field amplitude.

To illustrate the idea of this full coherent control, now consider a wedge that contains a line of nanosize scatterers (say, nanoparticles or nanoholes) located at the thick edge and parallel to it, i.e., in the x direction in Figure 1b. Consider first monochromatic light irradiating these nanoparticles or nanoholes that scatter and couple it into SPP wavelets. Every such scatterer emits SPPs in all directions; there is, of course, no favored directionality of the scattering. However, we assume that the excitation radiation and, correspondingly, the scattered wavelets of the SPP are coherent, and their phases smoothly vary in space along the thick edge, i.e., in the x direction. The SPP wavelets emitted by different scatterers will interfere, which in accord with the Huygens–Fresnel principle leads to formation of a smooth wavefront of the SPP wave at some distance from the scatterers in the far SPP field.

Such wavefronts are shown in Figure 1b with concave black curves. The energy of the SPP is transferred along the rays, which are lines normal to the wavefronts, shown by the colored lines. By the appropriate spatial phase modulation of the excitation radiation along the line of scatterers over distances of many SPP wavelengths, these wavefronts can be formed in such a way that the rays intersect at a given point, forming a nanofocus at the thin (sharp) edge of the wedge, as shown schematically in Figure 1b. Diffraction of the SPP waves will lead to a finite size of this focal spot that we will estimate later in this Letter.

By changing the spatial phase profile of the excitation radiation, this focal spot can be arbitrarily moved along the thin edge. This focusing and adiabatic concentration, as the SPPs slow down approaching the sharp edge, will lead to the enhancement of the intensity of the optical fields in the focal region. This dynamically controlled concentration of energy is a plasmonic counterpart of a large phased antenna array (also known as an aperture synthesis antenna or beamformer), widely used in radar technology and radio astronomy.[25] Now we can consider excitation by spatiotemporally shaped ultrashort pulses.[12,13] The field produced by them is a coherent superposition of waves with different frequencies whose amplitudes and phases can arbitrarily vary in space and with frequency. This modulation can be chosen so that all the frequency components converge at the same focal spot at the same time, forming an ultrashort pulse of the nanolocalized optical fields.

Turning to the theory, consider a nanofilm of metal in the xy plane whose thickness d in the z direction is adiabatically changing with the coordinate-vector $\boldsymbol{\rho} = (x,y)$ in the plane of the nanofilm. Let $\epsilon_m = \epsilon_m(\omega)$ be the dielectric permittivity of this metal nanofilm, and ϵ_d be the permittivity of the embedding dielectric. Because of the symmetry of the system, there are odd and even (in the normal electric field) SPPs. It is the odd SPP that is a slow-propagating, controllable mode. The dispersion relation for this mode defining its effective index $n(\boldsymbol{\rho})$ is

$$\tanh\left(\frac{1}{2}k_0 d(\boldsymbol{\rho})\sqrt{n(\boldsymbol{\rho})^2-\epsilon_m}\right) = -\frac{\epsilon_d\sqrt{n(\boldsymbol{\rho})^2-\epsilon_m}}{\epsilon_m\sqrt{n(\boldsymbol{\rho})^2-\epsilon_d}} \quad (1)$$

where $k_0 = \omega/c$ is the radiation wave vector in vacuum.

Let $\boldsymbol{\tau}$ be a unit tangential vector to the SPP trajectory (ray). It obeys an equation of ray optics[24] $n(\mathrm{d}\boldsymbol{\tau}/\mathrm{d}l) = \partial n/\partial\boldsymbol{\rho} - \boldsymbol{\tau}(\boldsymbol{\tau}\partial n/\partial\boldsymbol{\rho})$, where l is the length along the ray.

Now let us consider a nanofilm shaped as a nanowedge as in Figure 1b. In such a case, $n = n(y)$, and these trajectory equations simplify as $n(\mathrm{d}\tau_y/\mathrm{d}l) = \tau_x^2(\mathrm{d}n/\mathrm{d}y)$, $n(\mathrm{d}\tau_x/\mathrm{d}l) = -\tau_x\tau_y(\mathrm{d}n/\mathrm{d}y)$. From these, it follows that $n_x \equiv \tau_x n = \text{const}$. The SPP wave vector, related to its momentum, is $\mathbf{k}(\boldsymbol{\rho}) = k_0 n(\boldsymbol{\rho})\boldsymbol{\tau}$; this is the conservation of k_x (the transverse momentum). This allows one to obtain a closed solution for the ray. The tangent equation for the ray is $\mathrm{d}x/\mathrm{d}y = \tau_x/\tau_y$, where $\tau_y = \sqrt{1-n_x^2/n^2}$. From this, we get an explicit SPP ray equation as

$$x - x_0 = \int_{y_0}^{y}\left(\frac{n(y')^2}{n_x^{\,2}} - 1\right)^{-1/2}\mathrm{d}y' \quad (2)$$

where $\boldsymbol{\rho}_0 = (x_0,y_0)$ is the focal point where rays with any n_x converge. To find the trajectories, we use the real part of effective index (eq 1), as WKB suggests.

When the local thickness of the wedge is subwavelength ($k_0 d \ll 1$), the form of these trajectories can be found

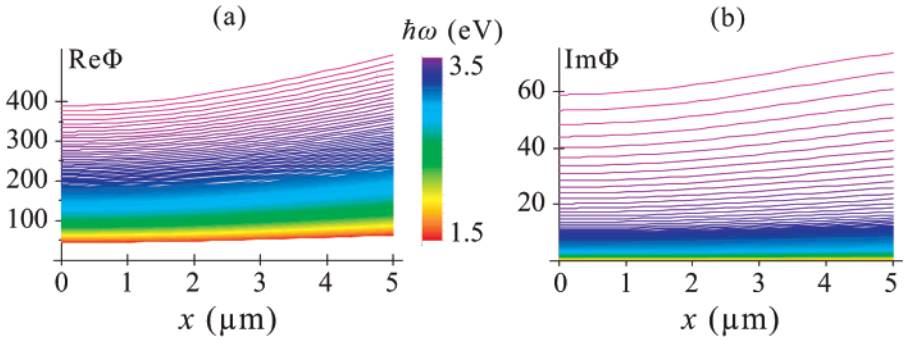

Figure 2. (a) Phase (real part of eikonal Φ) acquired by a SPP ray propagating between a point with coordinate x on the thick edge and the nanofocus, displayed as a function of x. The rays differ by frequencies that are color coded by the vertical bar. (b) The same as (a) but for extinction of the ray (Im Φ).

analytically. Under these conditions, dispersion relation (eq 1) has an asymptotic solution

$$n = \frac{n_a}{k_0 d} \qquad n_a = \ln \frac{\epsilon_m - \epsilon_d}{\epsilon_m + \epsilon_d} \tag{3}$$

Substituting this into eq 2, we obtain an explicit SPP ray equation $(x - x_0 - \sqrt{\bar{n}_a^2/n_x^2 - y_0^2})^2 + y^2 = \bar{n}_a^2/n_x^2$, where $\bar{n}_a = n_a/(k_0 \tan\theta)$, and $\tan\theta$ is the slope of the wedge. Thus, each SPP ray is a segment of a circle whose center is at a point given by $x = x_0 + \sqrt{(\bar{n}_a/n_x)^2 - y_0^2}$ and $y = 0$. This analytical result is in agreement with Figure 1b. If the nanofocus is at the sharp edge, i.e., $y_0 = 0$, then these circles do not intersect but touch and are tangent to each other at the nanofocus point.

As an example, we consider a silver[23] nanowedge illustrated in Figure 1b whose maximum thickness is $d_m = 30$ nm, the minimum thickness is $d_f = 4$ nm, and whose length (in the y direction) is $L = 5\ \mu$m. Trajectories calculated from eq 2 for $\hbar\omega = 2.5$ eV are shown by lines (color used only to guide eye); the nanofocus is indicated by a bold red dot. The different trajectories correspond to different values of n_x in the range $0 \le n_x \le n(L)$. In contrast to focusing by a conventional lens, the SPP rays are progressively bent toward the wedge slope direction.

The eikonal is found as an integral along the ray $\Phi(\boldsymbol{\rho}) = \int_{\boldsymbol{\rho}0}^{\boldsymbol{\rho}} \mathbf{n}(\boldsymbol{\rho})\ \mathbf{d}\boldsymbol{\rho}$. Consider rays emitted from the nanofocus (Figure 1b). Computed from this equation, the phases of the SPPs at the thick edge of the wedge (for $y = L$) are shown in Figure 2a as functions of the coordinate x along the thick edge. The colors of the rays correspond to the visual perception of the ray frequencies. The gained phase dramatically increases toward the blue spectral region, exhibiting a strong dispersion. The extinction for most of the frequencies except for the blue edge, displayed in Figure 2b, is not high.

Now consider the evolution of the field intensity along a SPP ray. For certainty, let SPPs propagate along the corresponding rays from the thick edge of the wedge toward the nanofocus as shown in Figure 1b. In the process of such propagation, there will be concentration of the SPP energy in all three directions (3D nanofocusing). This phenomenon differs dramatically from what occurs in conventional photonic ray optics.

To describe this nanofocusing, it is convenient to introduce an orthogonal system of ray coordinates whose unit vectors are $\boldsymbol{\tau}$ (along the ray), $\boldsymbol{\eta} = (-\tau_y, \tau_x)$ (at the surface normal to the ray), and $\mathbf{e}_z$ (normal to the surface). The concentration along the ray (in the $\boldsymbol{\tau}$ direction) occurs because the group velocity $v_g = [\partial(k_0 n)/\partial\omega]^{-1}$ of SPP asymptotically tends to zero (for the antisymmetric mode) for $k_0 d \to 0$ as $v_g = v_{0g} d$ where $v_{0g} = \text{const}$.[18] This contributes a factor $A_{\|} = 1/\sqrt{v_g(d)}$ to the amplitude of an SPP wave.

The compression of a SPP wave in the $\mathbf{e}_z$ (vertical) direction is given by a factor of $A_z = (\int_{-\infty}^{\infty} W\, dz)^{-1/2}$, where W is the energy density of the mode. Substituting a standard expression[24] for W, one obtains explicitly

$$A_z = \left(\frac{1}{8\pi}\exp(\mathrm{Re}\,\kappa_d d)\left\{\frac{\sinh(\mathrm{Re}\,\kappa_m d)}{\mathrm{Re}\,\kappa_m |\sinh(\kappa_m d/2)|^2}\left[1 + \frac{d(\omega \mathrm{Re}\,\epsilon_m)}{d\omega}\frac{|n|^2 + |\kappa_m|^2}{|\epsilon_m|^2}\right] - \frac{\sin(\mathrm{Im}\,\kappa_m d)}{\mathrm{Im}\,\kappa_m |\sinh(\kappa_m d/2)|^2}\left[1 + \frac{d(\omega \mathrm{Re}\,\epsilon_m)}{d\omega}\frac{|n|^2 - |\kappa_m|^2}{|\epsilon_m|^2}\right] + \frac{2}{\mathrm{Re}\,\kappa_d}\left[1 + \frac{|n|^2 + |\kappa_d|^2}{\epsilon_d}\right]\right\}\right)^{-1/2} \tag{4}$$

where $\kappa_m = k_0\sqrt{n - \epsilon_m}$ and $\kappa_d = k_0\sqrt{n - \epsilon_d}$. Note that the intensity distribution in Figure 1a is $I \propto (A_{\|} A_z)^{-2}$.

To obtain the compression factor $A_\perp$ for the $\boldsymbol{\eta}$ direction, we consider conservation of energy along the beam of rays corresponding to slightly different values of n_x. Dividing this constant energy flux by the thickness of this beam in the $\boldsymbol{\eta}$ direction, we arrive at

$$A_\perp = \left\{\left(1 - \frac{n_x^2}{n^2}\right)^{1/2} \int_{y_0}^{y} \frac{1}{n(y')}\left[1 - \frac{n_x^2}{n(y')^2}\right]^{-3/2} dy'\right\}^{-1/2} \tag{5}$$

The ray amplitude thus contains the total factor which describes the 3d adiabatic compression: $A = A_{\|} A_\perp A_z$.

Now consider the problem of coherent control. The goal is to excite a spatiotemporal waveform at the thick edge of the wedge in such a way that the propagating SPP rays converge at an arbitrary nanofocus at the sharp edge where

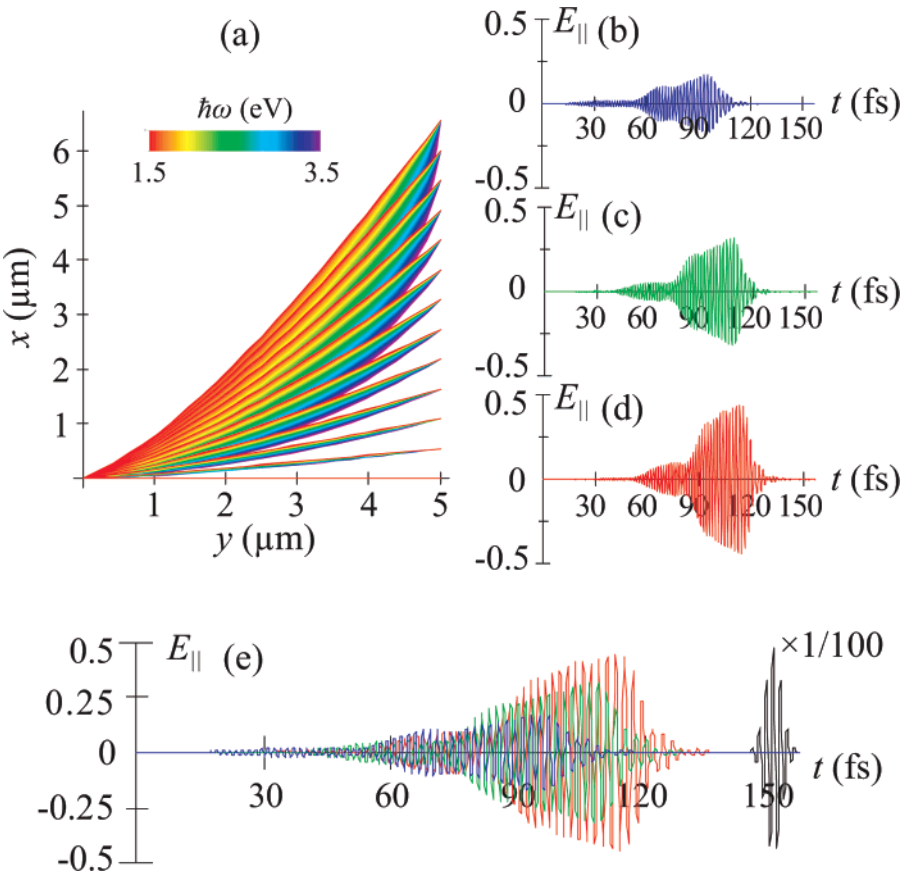

Figure 3. (a) Trajectories (rays) of SPP packets propagating from the thick edge to the nanofocus displayed in the *xy* plane of the wedge. The frequencies of the individual rays in a packet are indicated by color as coded by the bar at the top. (b−d) Spatiotemporal modulation of the excitation pulses at the thick edge of the wedge required for nanofocusing. The temporal dependencies (waveforms) of the electric field for the phase-modulated pulses for three points at the thick edge boundary: two extreme points and one at the center, as indicated, aligned with the corresponding *x* points at panel (a). (e) The three excitation pulses of panels (b−d) (as shown by their colors), superimposed to elucidate the phase shifts, delays, and shape changes between these pulses. The resulting ultrashort pulse at the nanofocus is shown by the black line. The scale of the electric fields is arbitrary but consistent throughout the figure.

an ultrashort pulse is formed. To solve this problem, we use the idea of back-propagation or time reversal.[26−28] We generate rays at the nanofocus as an ultrashort pulse containing just several oscillations of the optical field. By propagating these rays, we find amplitudes and phases of the fields at the thick edge at each frequency as given by the eikonal $\Phi(\boldsymbol{\rho})$. Then we complex conjugate the amplitudes of frequency components, which corresponds to the time reversal. We also multiply these amplitudes by exp(2Im Φ), which precompensates for the losses. This provides the required phase and amplitude modulation at the thick edge of the wedge.

We show an example of such calculations in Figure 3. Panel (a) displays the trajectories of SPPs calculated according to eq 2. The trajectories for different frequencies are displayed by colors corresponding to their visual perception. There is a very significant spectral dispersion: trajectories with higher frequencies are much more curved. The spatial-frequency modulation that we have found succeeds in bringing all these rays (with different frequencies and emitted at different *x* points) to the same nanofocus at the sharp edge.

The required waveforms at different *x* points of the thick edge of the wedge are shown in Figure 3b−d, where the corresponding longitudinal electric fields are shown. The waves emitted at large *x*, i.e., at points more distant from the nanofocus, should be emitted significantly earlier to precompensate for the longer propagation times. They should also have different amplitudes due to the differences in *A*. Finally, there is clearly a negative chirp (gradual decrease of frequency with time). This is due to the fact that the higher frequency components propagate more slowly and therefore must be emitted earlier to form a coherent ultrashort pulse at the nanofocus.

In Figure 3e, we display together all three of the representative waveforms at the thick edge to demonstrate their relative amplitudes and positions in time. The pulse at the extreme point in *x* (shown by blue) has the longest way to propagate and therefore is the most advanced in time. The pulse in the middle point (shown by green) is intermediate, and the pulse at the center ($x = 0$, shown by red) is last. One can notice also a counterintuitive feature: the waves propagating over longer trajectories are smaller in amplitude, although one may expect the opposite to compensate for the larger losses. The explanation is that the losses are actually insignificant for the frequencies present in these waveforms, and the magnitudes are determined by adiabatic concentration factor *A*.

Figure 3e also shows the resulting ultrashort pulse in the nanofocus. This is a transform-limited, Gaussian pulse. The propagation along the rays completely compensates the initial phase and amplitude modulation, exactly as intended. As a result, the corresponding electric field of the waveform is increased by a factor of 100. Taking the other component of the electric field and the magnetic field into account, the corresponding increase of the energy density is by a factor $\sim 10^4$ with respect to that of the SPPs at the thick edge.

Consider the efficiency of the energy transfer to the nanoscale. This is primarily determined by the cross section σ_{SPP} for scattering of photons into SPPs. For instance, for a metal sphere of radius R at the surface of the wedge, one can obtain an estimate $\sigma_{SPP} \sim R^6/(d_m^3 \lambda\!\!\!^{-})$, where $\lambda\!\!\!^{-}$ is the reduced photon wavelength. Setting $R \sim d_m$, we estimate $\sigma_{SPP} \sim 3$ nm^2. Assuming optical focusing into a spot of $\sim$300 nm radius, this yields the energy efficiency of conversion to the nanoscale of $\sim 10^{-3}$. Taking into account the adiabatic concentration of energy by a factor of 10^4, the optical field intensity at the nanofocus is enhanced by 1 order of magnitude with respect to that of the incoming optical wave.

The criterion of applicability of the WKB approximation is $\partial k^{-1}/\partial y \ll 1$. By substituting $k = k_0 n$ and eq 3, we obtain a condition $d_m/(n_a L) \ll 1$. This condition is satisfied everywhere including the nanofocus because $n_a \sim 1$ and $d_m \ll L$ for adiabatic grading. The minimum possible size of the wavepacket at the nanofocus in the direction of propagation, Δx, is limited by the local SPP wavelength: $\Delta x \sim 2\pi/k \approx 2\pi d_f/n_a$. The minimum transverse size a (waist) of the SPP beam at the nanofocus can be calculated as the radius of the first Fresnel zone: $a = \pi/k_x \geq \pi/(k_0 n_x)$. Because n_x is constant along a trajectory, one can substitute its value at the thick edge (the launch site), where from eq 3 we obtain $n_x \approx n = n_a/d_m$. This results in $a \approx \pi d_m/n_a$; thus a is on order of the maximum thickness of the wedge, which is assumed also to be on the nanoscale.

To briefly conclude, we have proposed and theoretically investigated an approach to full coherent control of spatiotemporal energy localization on the nanoscale. From the thick edge of a plasmonic metal nanowedge, SPPs are launched whose phases and amplitudes are independently modulated for each constituent frequency of the spectrum and at each spatial point of the excitation. This premodulates the departing SPP wave packets in such a way that they reach the required point at the sharp edge of the nanowedge in phase, with equal amplitudes forming a nanofocus where an ultrashort pulse with required temporal shape is generated. This system constitutes a "nanoplasmonic portal" connecting the incident light field whose features are shaped on the microscale, with the required point or features at the nanoscale.

Acknowledgment. This work was supported by grants from the Chemical Sciences, Biosciences, and Geosciences Division of the Office of Basic Energy Sciences, Office of Science, U.S. Department of Energy, a grant CHE-0507147 from NSF, and a grant from the U.S.−Israel BSF.

References

(1) Shapiro, M.; Brumer, P. *Phys. Rep.* **2006**, *425*, 195−264.
(2) Rabitz, H.; de Vivie-Riedle, R.; Motzkus, M.; Kompa, K. *Science* **2000**, *288*, 824−828.
(3) Apolonski, A.; Dombi, P.; Paulus, G. G.; Kakehata, M.; Holzwarth, R.; Udem, T.; Lemell, C.; Torizuka, K.; Burgdoerfer, J.; Hansch, T. W.; Krausz, F. *Phys. Rev. Lett.* **2004**, *92*, 073902-1−073902-4.
(4) Zeidler, D.; Staudte, A.; Bardon, A. B.; Villeneuve, D. M.; Dorner, R.; Corkum, P. B. *Phys. Rev. Lett.* **2005**, *95*, 203003-1−203003-4.
(5) Stockman, M. I.; Faleev, S. V.; Bergman, D. J. *Phys. Rev. Lett.* **2002**, *88*, 067402−1−4.
(6) Stockman, M. I.; Hewageegana, P. *Nano Lett.* **2005**, *5*, 2325−2329.
(7) Kubo, A.; Onda, K.; Petek, H.; Sun, Z.; Jung, Y. S.; Kim, H. K. *Nano Lett.* **2005**, *5*, 1123−1127.
(8) Kubo, A.; Pontius, N.; Petek, H. *Nano Lett.* **2007**, *7*, 470−475.
(9) Sukharev, M.; Seideman, T. *Nano Lett.* **2006**, *6*, 715−719.
(10) Sukharev, M.; Seideman, T. *J. Phys. B: At. Mol. Opt. Phys.* **2007**, S283−S298.
(11) Aeschlimann, M.; Bauer, M.; Bayer, D.; Brixner, T.; d. Abajo, F. J. G.; Pfeiffer, W.; Rohmer, M.; Spindler, C.; Steeb, F. *Nature* **2007**, *446*, 301−304.
(12) Wefers, M. M.; Nelson, K. A. *Opt. Lett.* **1993**, *18*, 2032−2034.
(13) Feurer, T.; Vaughan, J. C.; Nelson, K. A. *Science* **2003**, *299*, 374−377.
(14) Nomura, W.; Ohtsu, M.; Yatsui, T. *Appl. Phys. Lett.* **2005**, *86*, 181108-1−181108-3.
(15) Yin, L. L.; Vlasko-Vlasov, V. K.; Pearson, J.; Hiller, J. M.; Hua, J.; Welp, U.; Brown, D. E.; Kimball, C. W. *Nano Lett.* **2005**, *5*, 1399−1402.
(16) Verhagen, E.; Kuipers, L.; Polman, A. *Nano Lett.* **2007**, *7*, 334−337.
(17) Ropers, C.; Neacsu, C. C.; Elsaesser, T.; Albrecht, M.; Raschke, M. B.; Lienau, C. *Nano Lett.* **2007**, *7*, http://dx.doi.org/10.1021/nl071340m.
(18) Stockman, M. I. *Phys. Rev. Lett.* **2004**, *93*, 137404-1−137404-4.
(19) Stockman, M. I. Delivering Energy to Nanoscale: Rapid Adiabatic Transformation, Concentration, and Stopping of Radiation in Nano-Optics. In *Plasmonics: Metallic Nanostructures and Their Optical Properties II*; Halas, N. J., Huser, T. R., Eds.; SPIE: Denver, Colorado, 2004; Vol. 5512.
(20) Babajanyan, A. J.; Margaryan, N. L.; Nerkararyan, K. V. *J. Appl. Phys.* **2000**, *87*, 3785−3788.
(21) Maier, S. A.; Andrews, S. R.; Martin-Moreno, L.; Garcia-Vidal, F. J. *Phys. Rev. Lett.* **2006**, *97*, 176805−1−4.
(22) Gramotnev, D. K. *J. Appl. Phys.* **2005**, *98*, 104302−1−11.
(23) Johnson, P. B.; Christy, R. W. *Phys. Rev. B* **1972**, *6*, 4370−4379.
(24) Landau, L. D.; Lifshitz, E. M. *Electrodynamics of Continuous Media;* Pergamon: Oxford and New York, 1984.
(25) Mailloux, R. J. *Phased Array Antenna Handbook;* Artech House: Boston, 2005.
(26) Lerosey, G.; de Rosny, J.; Tourin, A.; Derode, A.; Montaldo, G.; Fink, M. *Phys. Rev. Lett.* **2004**, *92*, 193904-1−193904-3.
(27) Lerosey, G.; de Rosny, J.; Tourin, A.; Derode, A.; Fink, M. *Appl. Phys. Lett.* **2006**, *88*, 154101-1−154101-13.
(28) Lerosey, G.; de Rosny, J.; Tourin, A.; Fink, M. *Science* **2007**, *315*, 1120−1122.

NL071718G